SENSITIVITY OF LIDAR EQUATION SOLUTION TO BOUNDARY VALUES AND DETERMINATION OF THE VALUES

Qiu Jinhuan (邱金桓)

Institute of Atmospheric Physics, Academia Sinica, Beijing

Received October 10, 1986

ABSTRACT

An analytical dependence of the optical depth solution to lidar equation on boundary values was confirmed. According to the dependence this paper analyzed the sensitivity of lidar equation solutions obtained by forward and backward integration algorithms to the boundary values and quantitatively expounded an error limit to the boundary values under a given inversion accuracy. Furthermore, this paper presented a method for determination of the far-end boundary value in the case of inhomogeneous atmosphere, improving the accuracy of lidar equation solution.

I. INTRODUCTION

Lidar has been increasingly used in the atmospheric monitoring since 1960s. However, so far some theoretical difficulties in deriving quantitatively optical properties of cloud, fog and aerosol have not been solved yet. One is still confronted with a single equation having two unknowns, namely, the extinction coefficient and backscattering coefficient. For this reason, it is usually assumed that the extinction-to-backscattering ratio is constant along the path under consideration. Many authors studied the reasonableness of the assumption. Spinhirne et al. (1980) pointed out that except for the cases of local pollution and particle enlargement at high humidity, the aerosol extinction-to-backscattering ratio can be regarded as a constant in the boundary layer. Under the above assumption, the problem is reduced to determining boundary values. Analyzing the high sensitivity of lidar equation solution using the forward integration algorithm under the condition of low visibility to the near-end boundary value, Klett (1981) presented a backward integration algorithm. However, as pointed out by Fernald (1984) and Kastner et al. (1986), in the case of medium or high visibility, the backward integration algorithm is uncertain of having an advantage over the forward integration algorithm, and the accuracy in Klett's solution is closely associated with the error in the boundary value. Therefore, many authors (Fernald, 1984; Balin et al., 1986; Ferguson et al., 1983) have paid much attention to the study on selecting the boundary value. Most methods for determining the boundary value are based on the assumption of statistical homogeneity along the sounding path. However, the above studies do not deal with the question about how to justify the atmospheric homogeneity. As a matter of fact, the homogeneous assumption along a slant path is generally unsuitable. In one word, how to exactly select the boundary value is one of key problems about improving the accuracy in lidar equation solution. This paper has derived a quantitative dependence of the accuracy of lidar equation solution on the error in the boundary value, analyzed the suitableness of different methods

solving the lidar equation and presented a new approach to determinating the far-end boundary value, improving the accuracy of lidar equation solution.

II. SENSITIVITY OF LIDAR EQUATION TO BOUNDARY VALUES

The conventional lidar equation for the atmospheric sounding can be usually written as

$$V(r)=\frac{C_A\beta(r)}{r^2}e^{-2\int_0^r\sigma(r')dr'}, \tag{1}$$

where $V(r)$ is the lidar return signal from the atmosphere at the distance r; C_A is a constant of lidar system; $\beta(r)$ and $\sigma(r)$ are the atmospheric backscattering coefficient and the atmospheric extinction coefficient, respectively. The common way to account for the dependence between $\beta(r)$ and $\sigma(r)$ is to assume a power law relationship in the form

$$\beta(r)=B_0\sigma(r)^K, \tag{2}$$

where B_0 and K are constants.

Let $S(r)=V(r)r^2$, $\sigma_0=\sigma(r_0)$ and $\sigma_m=\sigma(r_m)$ with $r_0<r_m$. Then the solution to Eq. (1) with the forward integration algorithm reads

$$\sigma(r)=\frac{[S(r)/S(r_0)]^{1/k}}{\sigma_0^{-1}-\frac{2}{K}\int_{r_0}^{r}[S(r')/S(r_0)]^{1/k}dr'}, \tag{3}$$

while the backward integration algorithm reads

$$\sigma(r)=\frac{[S(r)/S(r_m)]^{1/k}}{\sigma_m^{-1}-\frac{2}{K}\int_{r}^{r_m}[S(r')/S(r_m)]^{1/k}dr'}, \tag{4}$$

where σ_0 and σ_m are near-end and far-end boundary values for two algorithms, respectively.

Let $\sigma^*(r)$ and $\tau^*(r_0,r_m)$ stand for the exact values of the extinction coefficient and optical depth, respectively, and $\tau(r_0,r_m)$ the optical depth solution, i.e.

$$\tau^*=\tau^*(r_0,r_m)=\int_{r_0}^{r_m}\sigma^*(r)dr,$$

$$\tau=\tau(r_0,r_m)=\int_{r_0}^{r_m}\sigma(r)dr.$$

Supposing that the noise of lidar signal $V(r)$ can be neglected and k=1, from Eq. (1) we get

$$S(r)/S(r_0)=\sigma^*(r)\exp\left[-2\int_{r_0}^{r}\sigma^*(r')dr'\right]/\sigma_0^*,$$

$$2\int_{r_0}^{r}S(r')/S(r_0)dr'=\left\{1-\exp\left[-2\int_{r_0}^{r}\sigma^*(r')dr'\right]\right\}/\sigma_0^*.$$

Then Eq. (3) can be changed into

$$\sigma(r)=\frac{\sigma^*(r)\exp\left[-2\int_{r_0}^{r}\sigma^*(r')dr'\right]/\sigma_0^*}{\sigma_0^{-1}-\left\{1-\exp\left[-2\int_{r_0}^{r}\sigma^*(r')dr'\right]\right\}/\sigma_0^*}$$

$$=\frac{\sigma^*(r)\exp\left[-2\int_{r_0}^{r}\sigma^*(r')dr'\right]}{\sigma_0^*/\sigma_0-\exp\left[-2\int_{r_0}^{r}\sigma^*(r')dr'\right]+1}.$$

Integrating the above equation over r yields

$$\int_{r_0}^{r_m}\sigma(r)dr=-\frac{1}{2}\int_{r_0}^{r_m}\frac{d\left[\exp\left(-2\int_{r_0}^{r}\sigma^*(r')dr'\right)\right]}{\sigma^*/\sigma_0+\exp\left[-2\int_{r_0}^{r}\sigma^*(r')dr'\right]-1}$$

$$=-\frac{1}{2}\ln(\sigma_0^*/\sigma_0)-\frac{1}{2}\ln[e^{-2\int_{r_0}^{r_m}\sigma^*(r)dr}+\sigma_0^*/\sigma_0-1],$$

$$\tau(r_0,r_m)=\frac{1}{2}\ln(\sigma_0^*/\sigma_0)+\frac{1}{2}\ln[e^{-2\tau^*(r_0,r_m)}+\sigma_0^*/\sigma_0-1]. \tag{5}$$

Define $X_0=\sigma_0/\sigma_0^*$, $R_0=R(X_0,\tau^*)=\tau(r_0,r_m)/\tau^*(r_0,r_m)$.
Then Eq. (5) can be rewritten as

$$R_0=R(X_0,\tau^*)=\left\{\ln\left[e^{-2\tau^*(r_0,r_m)}+\frac{1}{X_0}-1\right]+\ln X_0\right\}/2\tau^*(r_0,r_m). \tag{6}$$

Clearly, as $X_0=1$, $R_0=1$, i.e. $\tau(r_0,r_m)=\tau^*(r_0,r_m)$, implying that there is no error in the optical depth solution; as $X_0<1$, $R_0<1$ with the result that the solution is less than the exact value and as $X_0>1$, the solution is overestimated.

Similarly, the optical depth solution with backward integration algorithm is

$$\tau(r_0,r_m)=\frac{1}{2}\ln[e^{2\tau^*(r_0,r_m)}-\sigma_m^*/\sigma_m-1]-\ln(\sigma_m^*/\sigma_m), \tag{7}$$

and then

$$R_m=R(X_m,\tau^*)=\left\{\ln\left[e^{2\tau^*(r_0,r_m)}+\frac{1}{X_m}-1\right]+\ln X_m\right\}/2\tau^*(r_0,r_m), \tag{8}$$

with $X_m=\sigma_m/\sigma_m^*$ and $R_m=R(X_m,\tau^*)=\tau(r_0,r_m)/\tau^*(r_0,r_m)$.
Eq. (6) represents the dependence of the solution accuracy using the forward integration algorithm on the boundary value and Eq. (8) the backward integration algorithm.

The above-mentioned dependences can be clearly seen from Figs.1 and 2. As shown in Fig. 1, when X_0 changes between 0.8 and 1.2, R_0 is roughly linearly correlated with X_0 for $\tau^*(r_0,r_m)<0.5$ and $\Delta R_0\approx\Delta X_0$ for $\tau^*(r_0,r_m)<0.1$. Consequently, the relative error of the solution is equal to that of the boundary value. With increasing optical depth, the error in solution gets larger. For example, when the error of boundary values is larger than 2% ($X_0>1.02$) and $\tau^*(r_0,r_m)=2$, an unreasonably-negative extinction coefficient solution appears, and the value of $e^{-2\tau^*(r_0,r_m)}+\frac{1}{X_0}-1$ in Eq. (6) is also unreasonably negative, thus the curve $X_0=R(X_0,\tau^*)$ is ended. In order to get positive extinction coefficient solution, the errors in the boundary values must be less than 0.3% and 0.0006% for $\tau^*=3$ and $\tau^*=6$, respectively. Therefore, the forward integration algorithm is not suitable when $\tau^*>2$. However, the contrary is the case with the backward integral algorithm, as shown in Fig. 2. When X_m changes from 0.01 to 100 (four orders of magnitude), the error in optical depth solution is less than 40%, being insensitive to the boundary values. The sensitivity of the solution with the backward integration algorithm to the boundary values continuously gets stronger with decreasing optical depth. As $\tau^*(r_0,r_m)<0.5$, $\Delta R(X_m,\tau^*)\approx\Delta X_m$, thus the backward integration algorithm has no advantage over the forward ingration algorithm. Only when optical depth is larger than unity, would

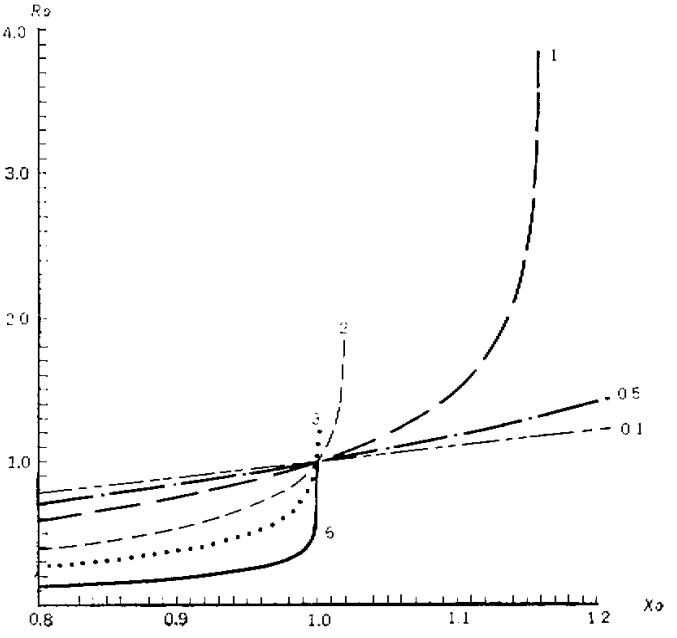

Fig. 1. Variation of R_0 with X_0 (Digits near curves denote optical depth).

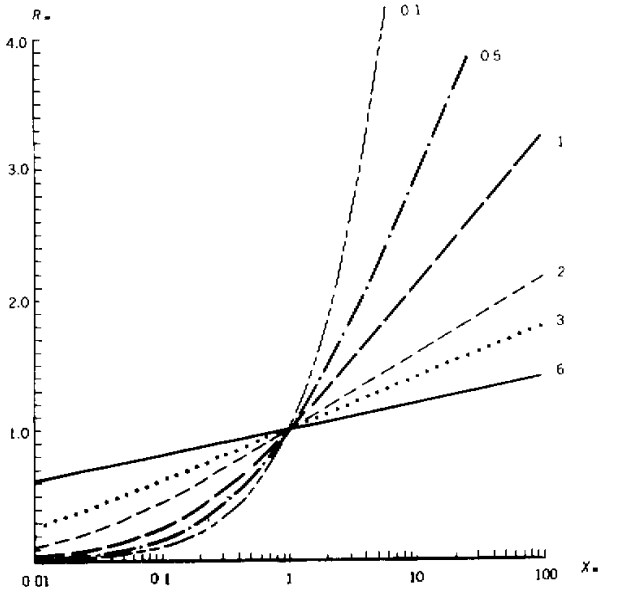

Fig.2 . Variation of R_m with X_m (Digits near curves denote optical depth).

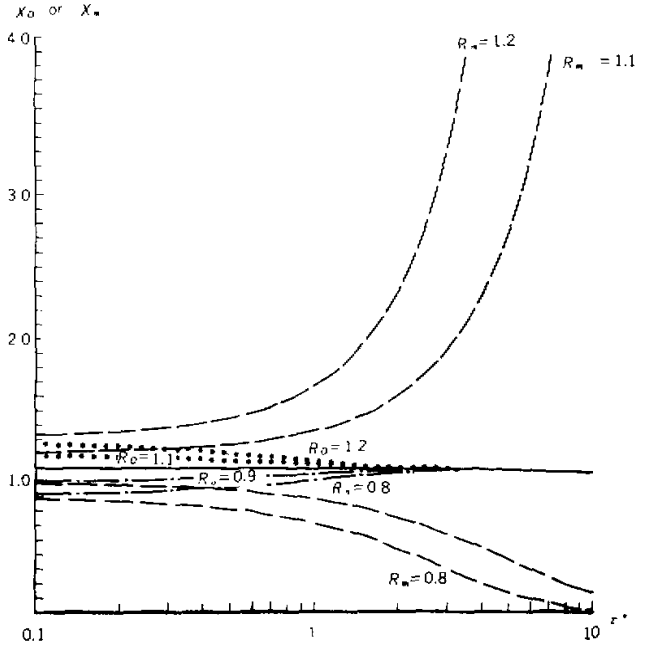

Fig. 3. A demand for the accuracy in boundary values under given retrieval accuracy.

the backward integration algorithm be more suitable because of the insensitivity of solution to boundary values.

Furthermore, it can be inferred from Eqs. (6) and (8)

$$X_0=(e^{-\tau R_0\tau^*}-1)/(e^{-\tau\tau^*}-1), \tag{9}$$

$$X_m=(e^{R_m\tau^*}-1)/(e^{2\tau^*}-1), \tag{10}$$

which can be used in estimating a error limit of boundary values under a demand for given retrieval accuracy. Fig. 3 shows variations of X_0 and X_m with τ^* for different R_0 and R_m. As $R_0=R_m$ there is always $|X_0-1|\leqslant|X_m-1|$ for any optical depth. Therefore if σ_0 and σ_m have the same relative error, the solution with backward integration algorithm is more exact than that with the forward integration algorithm. As shown in Fig. 3, X_0 approaches unity as a limit, but X_m diverges from unity with the increase of optical depth. Besides, $|X_0-1|\leqslant|R_0-1|$, $|X_m-1|\geqslant|R_m-1|$, which shows that the error in optical depth solution with the forward integration algorithm is larger than that of the boundary value and the contrary is the case with the backward integration algorithm.

An important use of lidar is to measure visibility. 10% measurement error in visibility at airport is generally demanded. For this purpose the error in optical depth must be less than 10% and a limit of errors in σ_0 and σ_m, shown in Table 1, is demanded, marked as $\delta\sigma_0$ and $\delta\sigma_m$ which are computed from Formulas (9) and (10). When $\tau^*>1$, $\delta\sigma_0<1.4\%$, but $\delta\sigma_m>26\%$. σ_0 is generally difficult to determine with so high accuracy, and thus the backward integration algorithm is more suitable. As $2.5\leqslant\tau^*\leqslant3$, the error in σ_m must

be less than 65%. Therefore, in order to enhance solution accuracy the more exact determination of σ_m is important, even for larger optical depth.

The above analysis also shows that the inversion error of lidar equation depends mainly on the relative error of boundary values rather than their absolute error. The solution stability depends on the magnitude of optical depth rather than extinction coefficient. In the case of smaller extinction coefficient, if optical depth is larger because of very long sounding distance, the solution with the backward integration algorithm will be still stable.

Table 1. Values $\delta\sigma_0$ and $\delta\sigma_m$ for Different Optical Depths

τ^*	≤0.1	0.1-0.3	0.3-0.5	0.5-0.7	0.7-1	1-1.5	1.5-2	2-2.5	2.5-3
$\delta\sigma_0$(%)	~10	7.1	5.5	4.3	2.8	1.4	0.62	0.27	0.11
$\delta\sigma_m$(%)	10	11	14	17	20	26	37	50	65

III. DETERMINATION OF BOUNDARY VALUE

It can be inferred from Eqs. (1) and (2) that

$$S(r) = C_A B_0 \sigma^k(r) e^{-2\int_0^r \sigma(r')dr'},$$

$$\int_{r_0}^{r_m} S(r)^{1/k}\,dr = (C_A B_0)^{1/k} \int_{r_0}^{r_m} \sigma(r) e^{-2\int_0^r \sigma(r')dr'/k}\,dr$$

$$= \frac{k}{2}(C_A B_0)^{1/k}\{\exp[-2\tau(0,r_0)/k]$$

$$-\exp[-2\tau(0,r_m)/k]\}, \tag{11}$$

$$\sigma_m = S(r_m)^{1/k}\exp[2\tau(0,r_m)/k]/(C_A B_0)^{1/k}. \tag{12}$$

By combining Eqs. (11) and (12), we have

$$\sigma_m = kS_m^{1/k}\{\exp[2\tau(r_0,r_m)/k] - 1\}/2\int_{r_0}^{r_m} S(r)^{1/k}dr. \tag{13}$$

If k is given, question can be summed up as determination of optical depth $\tau(r_0,r_m)$. Below we discuss two cases of horizontal and slant soundings, respectively.

1. *Horizontal Sounding*

In the horizontal sounding, a homogeneous atmosphere is usually supposed (Spinhirne, 1980; Lu Daren et al., 1976; Zhao Yanzeng et al., 1980). According to Balin's study (1986), in a statistically homogeneous atmosphere along the path, $\tau(r_0,r_m)$ can be determined by

$$\tau(r_0,r_m) = \frac{3}{2(r_m-r_0)^2}\int_{r_0}^{r_m}(r-r_0)\ln\frac{S(r_0)}{S(r)}dr. \tag{14}$$

Slope method is also suitable for the homogeneous atmosphere where extinction and backscattering coefficients are invariable along the path, marked as $\bar{\sigma}_0$ and $\bar{\beta}_0$, respectively. Then Eq. (1) can be changed into

$$g(r_i) = \ln S(r_i) = \ln(C_A\bar{\beta}_0) - 2\bar{\sigma}_0 r_i, \tag{15}$$

$$r_0 = r_1 < r_2 \cdots < r_i < \cdots < r_N = r_m,$$

with the solution $x = (A^TA)^{-1}g$,

where

$$x=[\ln(C_A\bar{\beta}_0),\ -2\bar{\sigma}_0]^T,$$

$$g=[g(r_1)\cdots g(r_N)]^T,$$

$$A^T=\begin{bmatrix}1 & 1 & \cdots & 1\\ r & r_2 & \cdots & r_N\end{bmatrix},$$

$$\bar{\sigma}_0=-\frac{1}{2}x_2,$$

$$\tau(r_1,r_m)=(r_m \quad r_1)\bar{\sigma}_0. \tag{16}$$

In the case of the homogeneous atmosphere, $g(r_i)$ in Formula (15) is linearly related with r_i but in fact, the fully homogeneous atmosphere does not exist. So in this paper the correlation coefficient R between $g(r)$ and r is used in indicating their linearity.

If $\tau(r_0,r_m)$ is determined with satisfactory accuracy, the boundary value $\sigma(r_m)$ can be computed as follows

$$t=S(r_m)/S'(r_m)=\frac{C_A\beta(r_m)e^{-2\tau(r_0,r_m)}}{C_A\bar{\beta}_0e^{-2(r_m-r_0)\bar{\sigma}_0}}\approx\frac{\sigma(r_m)}{\bar{\sigma}_0},$$

$$\sigma(r_m)=t\bar{\sigma}_0. \tag{17}$$

Table 2 compares the boundary values determined by different methods. In the table τ^* and σ_m^* are the exact optical depth and boundary value, $\tau^{(1)}$ and $\sigma_m^{(1)}$are the optical depth and boundary value derived from Formulas (13) and (14), $\tau^{(2)}$ and $\sigma_m^{(2)}$ by Formulas (16) and (13), respectively, $\sigma_m^{(3)}$ is the boundary value by Formula (17), $\sigma_m^{(3)}$ is equal to $\bar{\sigma}_0$ computed by the slope method, R is the correlation coefficient and No. stands for extinction coefficient distributions where No. 1–7 represent the distribution curves in Fig. 4 and No. 8–13 the curves in Figs. 5–7 respectively. For the uniform distribution No. 13 with $\sigma(r)\equiv 10$ in Fig. 7, the boundary values determined by different methods are all absolutely exact. For the six distributions marked as No. 1–6, being approximately regarded as homogeneous distribution with a random oscillation, the mean extinction coefficient changes from 0.8 (1/km) to 10 (1/km) with the corresponding visibility ranging 49 km to 0.4 km, and mean errors in $\sigma_m^{(1)}$, $\sigma_m^{(2)}$, $\sigma_m^{(3)}$, and $\sigma_m^{(4)}$ are 41.6%, 26.6%, 12.4% and 11.0%, respectively. The error of the boundary value determined by Formula (17) is the smallest and the value derived from Formulas (13) and (16) has got satisfactory accuracy, but the value from Formulas (13) and (14) has got the largest error, even as high as 100% or more. The distribution No. 7 with strong oscillation and distributions No. 8–12 with systematic variation can not be regarded as homogeneous, and hence correspond to the larger deviation of boundary values determined by above-mentioned methods. Generally speaking, the error in $\sigma_m^{(2)}$ is the largest and $\sigma_m^{(1)}$ with the slope method smaller. A homogeneous atmosphere will lead to the correlation coefficient equal to unity ($R=1$). However, it can be seen from Table 2 that the values of R for inhomogeneous distributions marked as No. 8–12 are uncertainly less than those for No. 1–6. Therefore, the linearity of $\ln S(r)$ with r can not be considered as an unique criterion on homogeneity of atmosphere. The above analysis shows that the boundary values derived from Formula (17) or Formulas (13) and (16) are more exact under the condition of statistically-homogeneous atmosphere. In the up-slant path sounding, a larger systematic variation of extinction coefficient with height may lead to larger error in boundary values determined by above-mentioned methods.

Table 2. Comparison of Boundary Values and Optical Depths Determined with Different Methods

No.	τ^*	$\tau^{(1)}$	$\tau^{(2)}$	σ_m^*	$\sigma_m^{(1)}$	$\sigma_m^{(2)}$	$\sigma_m^{(3)}$	$\sigma_m^{(4)}$	R	$\sigma_m^{(5)}$	$\tau^{(5)}$
1	1.94	1.98	1.96	9.81	10.5	9.81	10.3	8.96	0.643		
2	1.51	1.68	1.59	3.24	4.55	3.98	3.76	3.62	0.845		
3	1.01	1.14	0.998	0.742	0.963	0.988	0.961	0.737	0.827		
4	0.90	1.02	0.906	0.403	0.574	0.604	0.411	0.474	0.793		
5	0.418	0.356	0.435	0.273	0.222	0.218	0.289	0.266	0.617		
6	0.211	0.335	0.238	0.090	0.189	0.119	0.105	0.112	0.350		
7	0.150	0.547	0.305	0.088	0.578	0.137	0.207	0.322	0.238		
8	0.169	1.40	1.22	0.024	0.996	0.609	0.664	0.654	0.802	0.025	0.163
9	1.34	0.757	1.18	0.358	0.094	0.402	0.247	0.299	0.779	0.254	1.19
10	1.78	0.538	1.65	1.121	0.064	1.47	0.841	0.387	0.583	0.884	1.66
11	0.765	1.694	0.758	0.294	2.19	0.981	0.29	1.28	0.732	0.277	0.760
12	1.41	2.69	2.38	1.22	18.4	6.79	8.48	8.54	0.67	1.00	1.27
13	2.70	2.70	2.79	10.0	10.0	10.0	10.0	10.0	1.0	99.2	3.88

2. *Slant-Path Sounding*

In the case of inhomogeneous atmosphere, new information must be introduced in order to determine the far-end boundary value because of two unknowns in lidar equation. Then, horizontal lidar return signal is added to infer the boundary value σ_m when slant-path sounding.

Let $S(r)$, $\sigma(r)$ and $\bar{\tau}$ represent the horizontal lidar return signal, extinction coefficient and optical depth, we have

$$\int_{r_0}^{r_m} S(r)^{1/k}dr = \frac{k}{2}(C_A B_0)^{1/k}\{\exp[-2\bar{\tau}(r_0, r_m)/k] - \exp[-2\bar{\tau}(0, r_m)/k]\}. \quad (18)$$

Suppose that the values B and k in the slant direction are equal to those in the horizontal direction, we have

$$\int_{r_0}^{r_m} S(r)^{1/k}dr = \frac{k}{2}(C_A B_0)^{1/k}\{\exp[-2\tau(0, r_0)/k] - \exp[-2\tau(0, r_m)/k]\}. \quad (19)$$

Combining Eqs. (18) with (19) leads to

$$\int_{r_0}^{r_m} S(r)^{1/k}dr \Big/ \int_{r_0}^{r_m} S(\bar{r})^{1/k}dr = \{\exp[-2\tau(0, r_0)/k] - \exp[-2\tau(0, r_m)/k]\}/\{\exp[-2\bar{\tau}(0, r_0)/k] - \exp[-2\bar{\tau}(0, r_m)/k]\}, \quad (20)$$

$$1 - \exp[-2\tau(r_0, r_m)/k] = \{1 - \exp[-2\bar{\tau}(r_0, r_m)/k]\}f/C, \quad (21)$$

$$\tau(r_0, r_m) = -\frac{k}{2}\ln\{1 - [1 - \exp(-2\bar{\tau}/k)]f/C\}, \quad (22)$$

where $C=\exp[-2\tau(0,r_0)/k]/\exp[-2\bar{\tau}(0,r_0)/k]$,

$$f=\int_{r_0}^{r_m}S(r)^{1/k}dr/\int_{r_0}^{r_m}\overline{S(r)}^{1/k}dr.$$

If r_0 is small or there is a smaller variation in the extinction coefficient with the range of $0\leqslant r\leqslant r_0$, then $\tau(0,r_0)\approx\bar{\tau}(0,r_0)$, and hence $C\approx 1$. Hereafter, $C=1$ is considered.

If there are no cloud and fog and no local pollution source in the boundary layer, $k=1$ is usually suitable.

According to Klett's study (1985), the extinction-to-backscattering ratio in low cloud or fog is greatly different from that in aerosol layer. In this case, setting k to be equal to unity and then computing the optical depth from Formula (22) can lead to large error of inversion. According to Klett's another paper (1981), the forward integration algorithm is very sensitive to the error of k for the larger optical depth. The characteristic can be used in determining the value of k. The solution at $r=r_m$ with forward integration algorithm is

$$\sigma(r_m)=[S(r_m)/S(r_0)]^{1/k}/\left\{\sigma_0^{-1}-\frac{2}{k}\int_{r_0}^{r_m}[S(r)/S(r_0)]^{1/k}dr\right\}. \tag{23}$$

In order to get a positive solution, k must satisfy the condition

$$\sigma_0^{-1}-\frac{2}{k}\int_{r_0}^{r_m}[S(r)/S(r_0)]^{1/k}dr>0,$$

or

$$g(k)=1-\frac{2\sigma_0}{k}\int_{r_0}^{r_m}[S(r)/S(r_0)]^{1/k}dr>0. \tag{24}$$

For the larger optical depth, $g(k)$ approaches zero, and thus a slight deviation of k from the exact value can lead to unsatisfaction of Eq. (24). In this paper the solution of k is considered as the value which satisfies

$$0<g(k)\leqslant 0.02. \tag{25}$$

The results of numerical experiment in the case of $k=1$ are shown in Figs. 5-7, where $r_0=0.01$ km, $C=1$, and horizontal extinction coefficient distributions in Figs. 5-7 are respectively taken to be distribution curves 5, 3 and 1 in Fig. 4 with $\bar{\sigma}_0$ being 0.2, 1 and 10 (1/km). First, $\tau(r_0,r_m)$ is determined from Eq. (22), then the boundary value $\sigma_m^{(5)}$ from Eq. (13) and the optical depth $\tau^{(5)}$ from Eq. (4). All these are listed in table 2. The observations $V(r)$ are assumed to have randon errors with a maximum of 10% in numerical tests. As shown in the figures except for distribution 2 in Fig. 7, this treatment reasults in satisfactory numerical tests in which $\sigma_m^{(5)}$ has much higher accuracy than $\sigma_m^{(1)}$, $\sigma_m^{(2)}$, $\sigma_m^{(3)}$ and $\sigma_m^{(4)}$ and the error in $\tau^{(5)}$ is less than 12% (see Table 2). For distribution 2 in Fig. 7, $\sigma_m^{(5)}$ is approximately one order of magnitude larger than the exact value, thus the solution has larger error, which is due to the fact that larger optical depth of $\tau^*(r_0,r_m)=2.7$ leads to the larger error in $\tau(r_0,r_m)$ computed from Eq. (22). This point can be clearly seen from the following analysis.

Let

$$y=\{1-\exp[-2\bar{\tau}(r_0,r_m)/k]\}f/C.$$

Then Eq. (21) can be changed into

$$\frac{d\tau}{\tau}=\frac{k\{1-\exp[-2\tau(r_0,r_m)/k]\}}{2\tau(r_0,r_m)\exp[-2\tau(r_0,r_m)/k]}\frac{dy}{y}.$$

When $\tau(r_0, r_m) \gg 1$, $1 - \exp[-2\tau(r_0, r_m)/k] \approx 1$, and hence we have in the case of $k = 1$

$$\frac{d\tau}{\tau} \approx \frac{\exp[2\tau(r_0, r_m)/k]}{2\tau(r_0, r_m)} \frac{dy}{y} = A\frac{dy}{y},$$

$$A = \exp[2\tau(r_0, r_m)]/2\tau(r_0, r_m). \tag{27}$$

Table 3 shows the value of A for different optical depths. When $\tau(r_0, r_m) \geq 1$, A rapidly increases with the increase of τ. For example, as $\tau = 2.7$, $A = 41$, which implies that 1% error in y would lead to 41% error in optical depth solution, and as $\tau = 2$, $A = 13.6$ thus, as $\tau \leq 2$, if the error in y is less than 1%, the error in $\tau(r_0, r_m)$ computed from Formula (22) is less than 14%. For very large optical depth Formula (22) is not suitable.

Table 3. Variation of A with τ

τ	1	1.5	2	2.5	2.7	3	4	5
A	3.7	6.7	13.6	29.7	41.0	67.2	372.6	2203

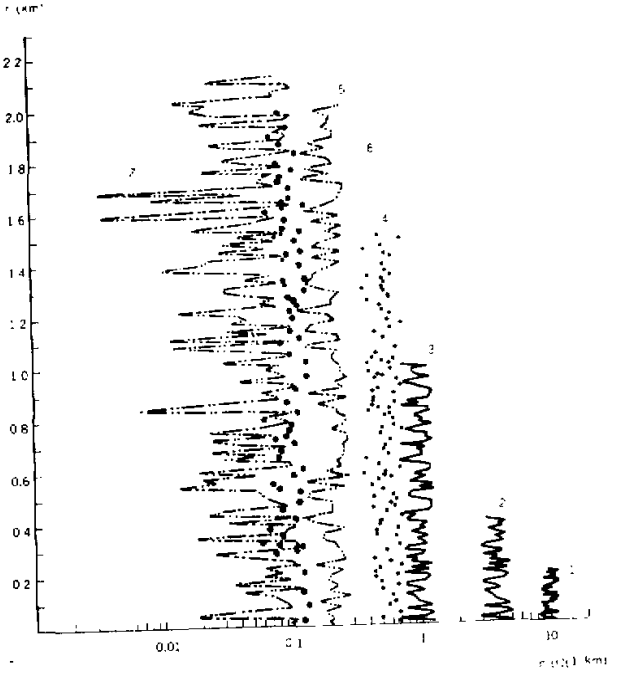

Fig. 4. Extinction coefficient distributions.

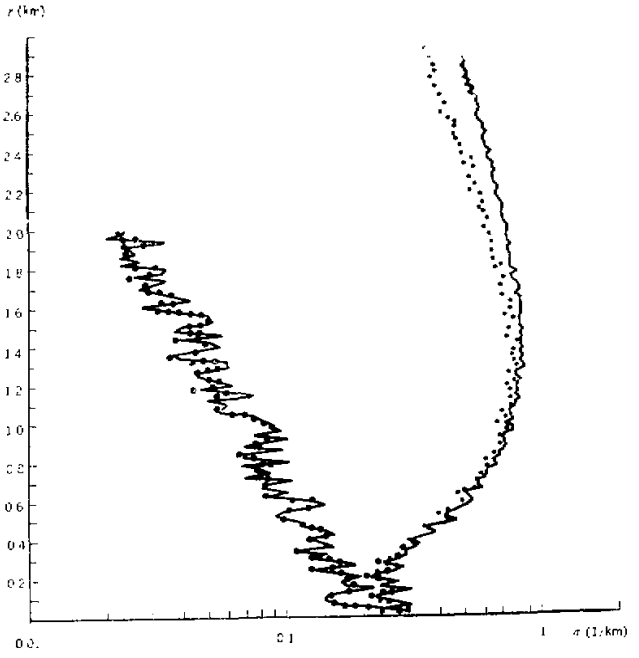

Fig. 5. Inversion results (dotted lines) of extinction coefficient distribution (solid lines) under high visibility.

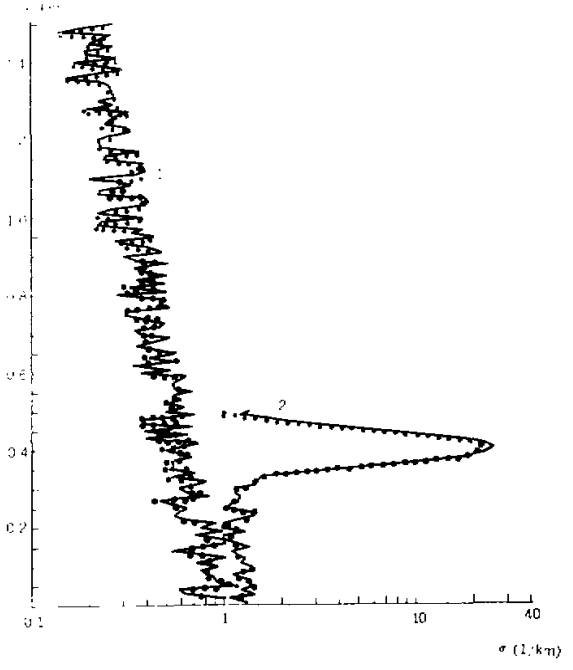

Fig. 6. Inversion results (dotted lines) of extinction coefficient distribution (solid lines) under medium visibility.

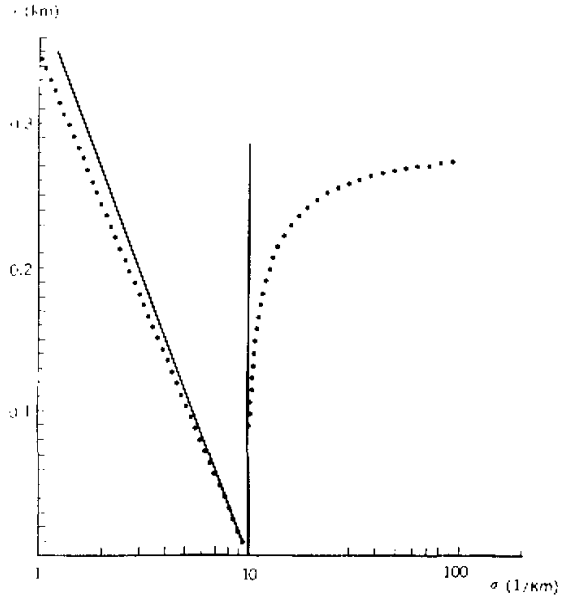

Fig. 7. Inversion results (dotted lines) of extinction coefficient distribution (solid lines) under low visibility.

The results of numerical experiments in the case of $k \neq 1$ are shown in Tables 4 and 5, where the extinction coefficient distribution is taken to be distribution 2 in Fig. 6 with a cloud layer at the height of 0.4 km and the exact values of k and optical depth are 1.34 and 1.78 respectively. As shown in Table 4, when $k<1.28$, an unreasonably negative $g(k)$ and the solution with the forward integration algorithm are obtained. As $k=1.29$, $g(k)=0.013$, satisfying Eq. (25). Therefore it is selected as the solution. In Table 5, σ_m^* is the exact boundary value, $\sigma_m^{(1)}$ and $\sigma_m^{(2)}$ are boundary values computed from Eqs. (22) and (13) under the assumption of $k=1$ and $k=1.29$ respectively. As $k=1$, $\sigma_m^{(1)}=-0.04$, being unreasonably negative, and as $k=1.29$, $\sigma_m^{(2)}=1.95$ which corresponds to the optical depth solution of 2.08 and the solution error of 16.9%. Evidently, the solution with $k=1.29$ is much more reasonable than that with $k=1$.

Table 4. Variation of Function $g(k)$ with k

k	1	1.1	1.2	1.24	1.28	1.29	1.30	1.34	1.4	1.5
$g(k)$	−0.625	−0.331	−0.125	−0.061	−0.035	0.013	0.024	0.079	0.133	0.22

Table 5. Boundary Value and Optical Depth Solution

σ_m^*	$\sigma_m^{(1)}$	$\sigma_m^{(2)}$	τ^*	$\tau^{(2)}$
1.093	−0.04	1.95	1.78	2.08

IV. CONCLUSIONS

(1) According to the dependence introduced in this paper of the optical depth solution to lidar equation on the boundary value, the solving stability of lidar equation depends mainly on the magnitude of the optical depth rather than extinction coefficient and the solution accuracy depends on the relative error in the boundary value. The error in optical depth solution with forward integration algorithm is always more than the error in boundary values and with increase of optical depth it gets more sensitive to the latter. When the error in boundary values is within 3%, only for optical depth less than unity, the solution to lidar equation with the forward integration algorithm will be reliable. The contrary is the case with the backward integration algorithm, i.e. the error in optical depth solution is always less than the error in boundary values, and the larger the optical depth is, the less sensitive to the latter error the solution is.

(2) Under the condition of the statistical homogeneity along the horizontal path, first we find the mean value of extinction coefficient by slope method and then determine the boundary value from Eq. (17) or (13). As slant-path sounding, the assumption of the statistical homogeneity along the path and hence all methods for determing the boundary value based on the assumption are generally unsuitable. In this case, if new information is not introduced, the far-end boundary value can not be exactly determined and it is difficult to justify the atmospheric homogeneity according to slant lidar return signals. In this paper, a method for determining the far-end boundary value in the slant direction through introducing horizontal lidar return information is presented. Numerical experiments show that the method is suitable for different extinction coefficient distributions with the optical depth less than 2. As optical depth is very large, the method can lead to unreasonable solution. In fact, lidar penetrating capacity is generally within a limit of the optical depth equal to 2.

(3) As the optical depth is larger, the solution with the forward integration algorithm is very sensitive to the value of k. The characteristic can be used in determining k with the error less than 5% for the optical depth larger than 1.8.

REFERENCES

Balin, Yu. S. et al. (1986), Lidar measurements of slant visual range, Abstracts of 13th ILRC, 38–40.

Ferguson, J. A. and Stephens, D. H. (1983), Algorithm for inverting lidar returns, *Appl. Opt.*, **22**:3673–3675.

Fernald, F. G. (1984), Analysis of atmospheric lidar observations: some comments, *Appl. Opt.*, **23**:652.

Hargard, A. (1986), Extinction and visibility measurements in the lower atmosphere with UV-YAG-lidar, Abstracts of 13th ILRC, 32–33.

Kastner, M. and Quenzel H. (1986), The usefulness of Klett's inversion algorithms to simulated satellite lidar returns, Abstracts of 13th ILRC, 24–27.

Klett, J. D. (1981), Stable analytical inversion solution for processing lidar returns, *Appl. Opt.*, **20**:211–220.

Klett, J. D. (1985), Lidar inversion with variable backscatter/extinction ratios, *Appl. Opt.*, **24**:1638–1643.

Lu Daren et al. (1976), An experimental study of visibility by lidar, *Scientia Atmospherica Sinica*, **1**:55–61 (in Chinese).

Qiu Jinhuan et al. (1987), Remote sensing and analyzing of atmospheric aerosol optical property in Beijing, *Acta Meteorologica Sinica*, **45**:(in Chinese with English abstract).

Spinhirne, J. D., et al. (1980), Vertical distribution of aerosol extinction cross section and inference of aerosol imaginary index in the troposphere by lidar technique, *J. Appl. Meteor.*, **19**:426–438.

Zhao Yanzeng et al. (1980), An experiment of slant visibility measurement by lidar, *Scientia Atmospherica Sinica*, **4**:168–175 (in Chinese with English abstract).